Open Charm Spectroscopy and Mass Measurements in LHCb.

Antimo Palano

INFN and University of Bari, Italy

on behaf of the LHCb Collaboration

Outline:

- New results on charm spectroscopy.
- Results on strange charm spectroscopy.
- Accurate measurement of the D masses.

CHARM 2013, August 31-September 4 2013, Manchester, UK

Charm meson spectroscopy

□ The quark model predicts many states with different quantum numbers in limited mass regions (Godfrey and Isgur, Phys.Rev.D32",189 (1985)).

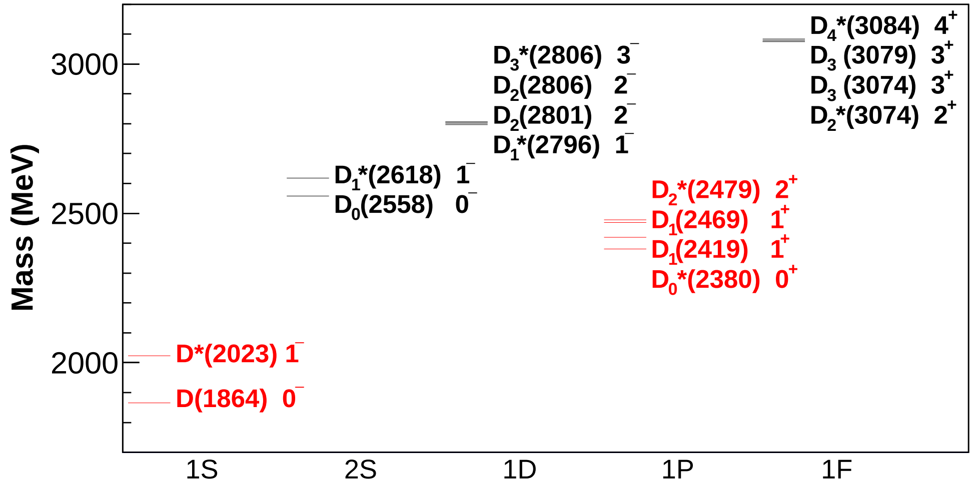

□ The ground states (D, D^*), and two of the 1P states, $D_1(2420)$ and $D_2^*(2460)$, are experimentally well established since they have relatively narrow widths (∼30 MeV).

□ The broad $L = 1$ states, $D_0^*(2400)$ and $D_1'(2430)$, have been established by the Belle and BaBar experiments in exclusive B decays.

□ *BaBar experiment has recently found four new states decaying to* $D\pi$ *and* $D^*\pi$ *(Phys.Rev.D82,111101(2010))*.

□ **Very complex experimental environment which require confirmation**.

Channels and Dataset

□ We reconstruct the following final states (arXiv:1307.4556):

$\mathbf{pp} \rightarrow \mathbf{X} \quad \pi^{-}\mathbf{D}^{+}$
$\qquad\qquad\qquad \rightarrow K^{-}\pi^{+}\pi^{+}$

$\mathbf{pp} \rightarrow \mathbf{X} \quad \pi^{+}\mathbf{D}^{0}$
$\qquad\qquad\qquad \rightarrow K^{-}\pi^{+}$

$\mathbf{pp} \rightarrow \mathbf{X} \quad \pi^{-}\mathbf{D}^{*+}$
$\qquad\qquad\qquad \rightarrow \pi^{+}D^{0}$
$\qquad\qquad\qquad\qquad \rightarrow K^{-}\pi^{+}$

at 7 TeV, where **X** represents any collection of charged and neutral particles.

□ The analysis based on ($\approx 1\ fb^{-1}$) of data.

□ D^{+}, D^{0}, and D^{*+} signals.

The use of charge-conjugate decay modes is implied.

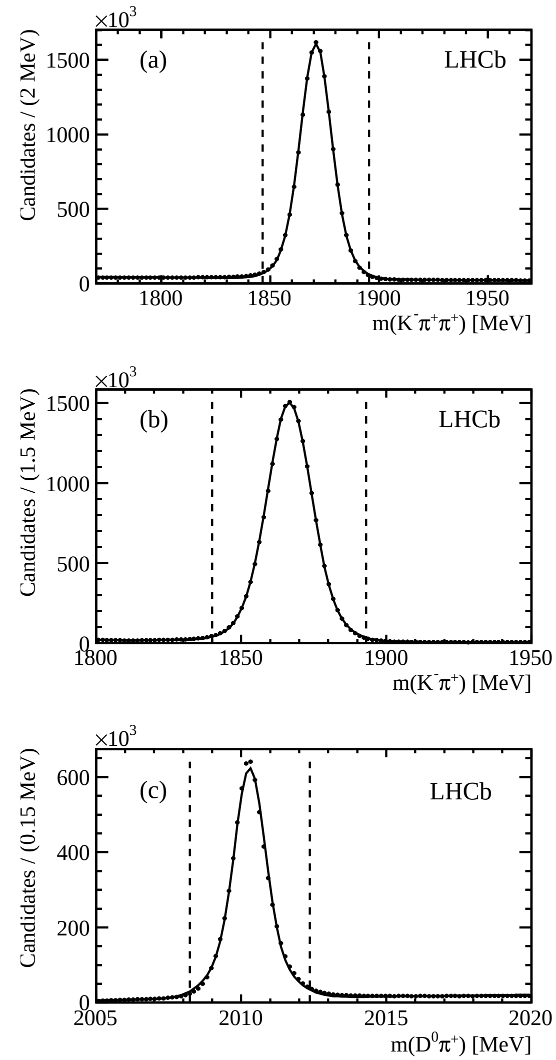

Data selection.

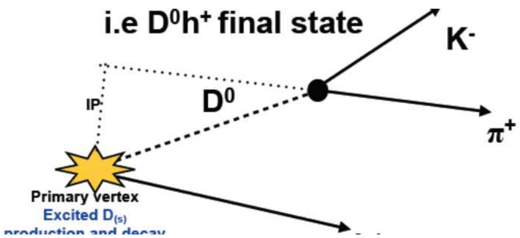

□ Reconstructed D and D^* are combined with another hadron pointing to the same primary vertex.

□ Large combinatorial background removed requiring $cos\theta > 0$.

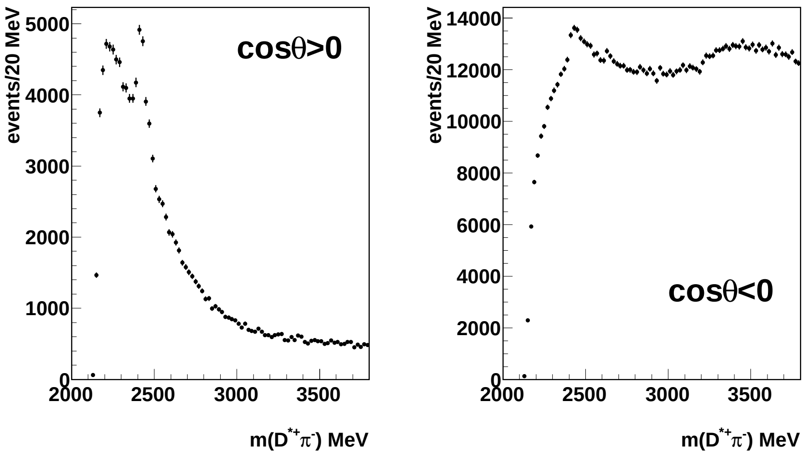

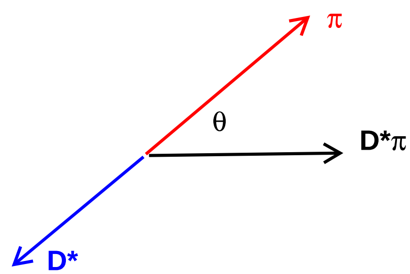

□ **Apply a cut at $p_T > 7.5$ GeV/c for all final states.**

□ $7.9{\times}10^6$, $7.5{\times}10^6$ and $2.1{\times}10^6$ $D^+\pi^-$, $D^0\pi^+$ and $D^{*+}\pi^-$ candidates are obtained.

Experimental resolution and efficiency

□ We obtain mass resolution ≈ 4 MeV at the $D_2^*(2460)$ mass similar for all the channels.

□ Resolution effects negligible when compared to the widths of the resonances under study.

□ The $D^{*+}\pi^-$ final state gives information on the spin-parity assignment of a given resonance.

□ In the rest frame of the $D^{*+}\pi^-$, we define the ahelicity ngle θ_H as the angle between the π^- and the π^+ from the D^{*+} decay.

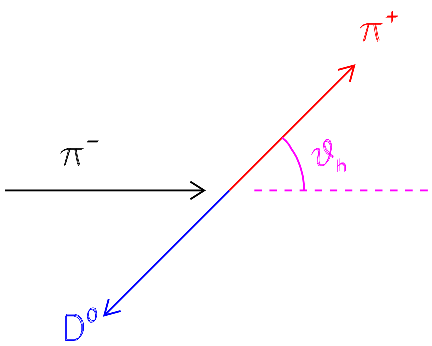

□ We compute the efficiency as a function of the helicity angle θ_H and find it uniform.

$D^+\pi^-$ and $D^+\pi^+$ mass spectra.

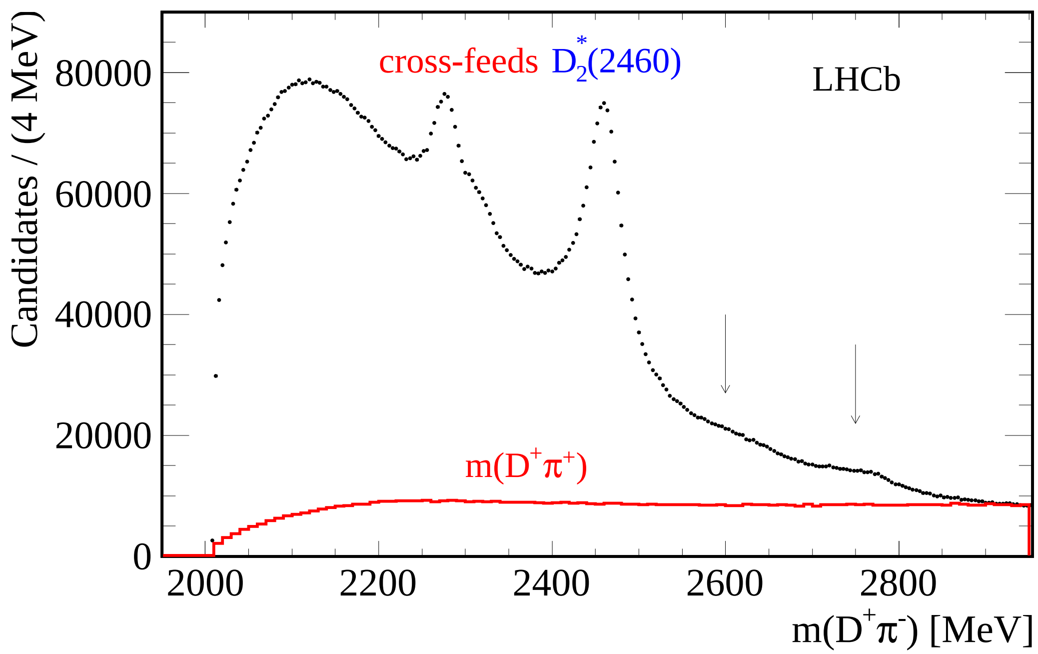

- The $D^+\pi^-$ mass spectrum shows a cross-feed from the decay

$$D_1(2420)^0 \text{ or } D_2^*(2460)^0 \to \pi^- D^{*+}(\to D^+\pi^0/\gamma)\ (32.3\%)$$

  where the π^0/γ is not reconstructed.

- Strong $D_2^*(2460)^0$ signal and weak structures around 2600 and 2750 MeV.
- The wrong-sign $D^+\pi^+$ mass spectrum does not show any structure.

$D^0\pi^+$ and $D^0\pi^-$ mass spectra.

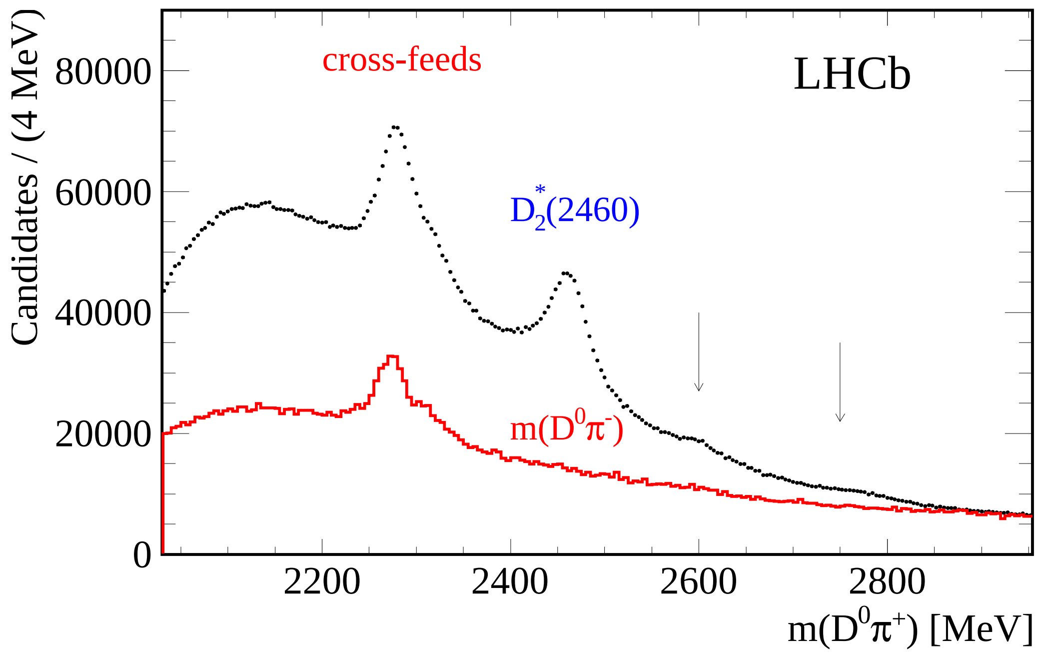

- The $D^0\pi^+$ mass spectrum shows a cross-feed from the decays:

$$D_1(2420)^+ \text{ or } D_2^*(2460)^+ \to \pi^+ D^{*0} \quad (\to D^0\pi^0)\ (61.9\%)$$

$$(\to D^0\gamma)\ (38.1\%)\ .$$

- Strong $D_2^*(2460)^+$ signal and weak structures around 2600 and 2750 MeV.
- The wrong-sign $D^0\pi^-$ mass spectrum shows cross-feeds from:

$$D_1(2420)^0 \text{ or } D_2^*(2460)^0 \to \pi^- D^{*+}(\to D^0\pi^+)\ (67.7\%)$$

$D^{*+}\pi^-$ and the $D^{*+}\pi^+$ mass spectra.

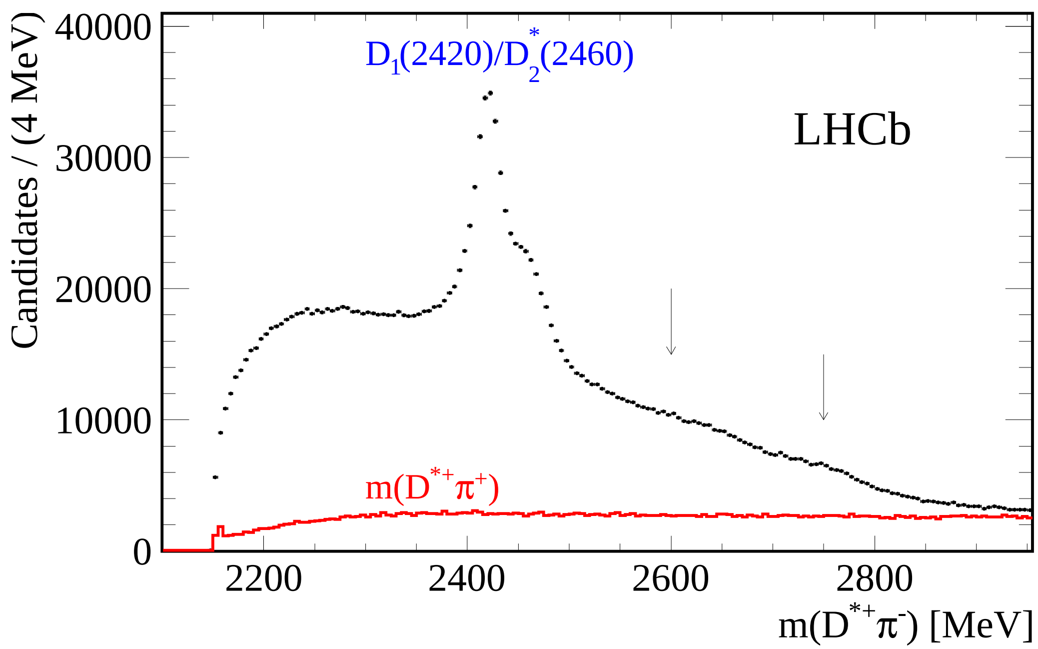

- The $D^{*+}\pi^-$ mass spectrum is dominated by the presence of the $D_1(2420)^0$ and $D_2^*(2460)^0$ signals.
- At higher mass, complex broad structures in the mass region between 2500 and 2800 MeV.
- The wrong-sign $D^{*+}\pi^+$ mass spectrum does not show any structure.
- No cross-feeds in this final state.

Study of the $D^{*+}\pi^-$ angular distributions.

□ Expected angular distributions for different spin assignments and MC simulations.

J^P	Helicity Distribution
0^+	decay not allowed
1^-	$\propto \sin^2\theta_H$
2^+	$\propto \sin^2\theta_H$
3^-	$\propto \sin^2\theta_H$
0^-	$\propto \cos^2\theta_H$
1^+	$\propto 1 + h\cos^2\theta_H$
2^-	$\propto 1 + h\cos^2\theta_H$

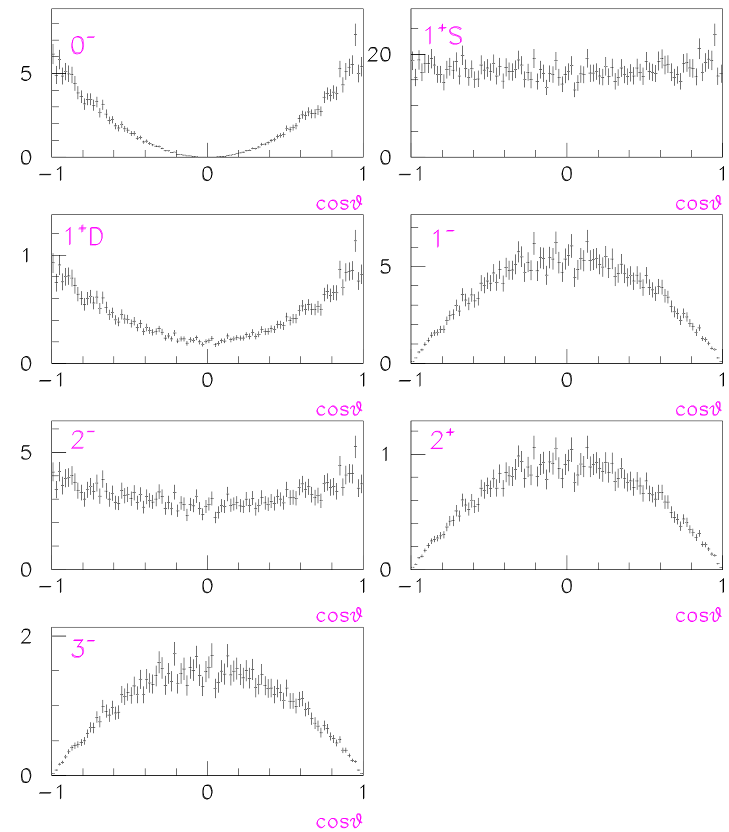

□ States having $J^P = 0^+, 1^-, 2^+, 3^-, ..$ are defined as having "Natural Parity".

□ States having $J^P = 0^-, 1^+, 2^-, ...$ are defined as having "Unnatural Parity".

□ A resonance decaying to $D\pi$ has "Natural Parity".

Study of the $D^{*+}\pi^-$ angular distributions.

□ We divide the data into three samples:

$|\cos\theta_H| > 0.75$, **Enhanced Unnatural Parity Sample.**
$(0.55 \times 10^6$ events, Natural Parity suppressed by a factor 11.6)

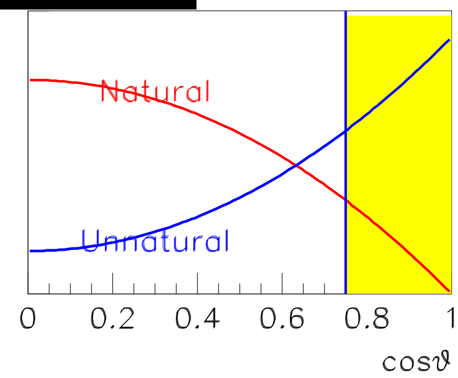

$|\cos\theta_H| < 0.5$, **Natural Parity Sample.**
$(0.98 \times 10^6$ events, Natural Parity suppressed by a factor 1.5)

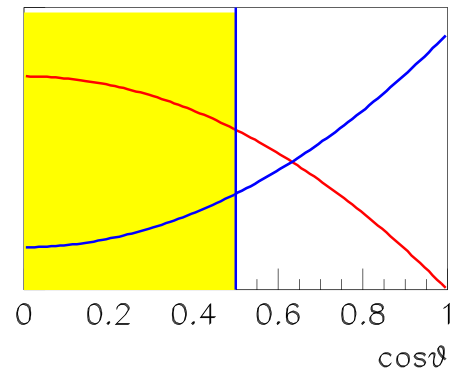

$|\cos\theta_H| > 0.5$, **Unnatural Parity Sample.**
$(1.06 \times 10^6$ events, Natural Parity suppressed by a factor 3.2)

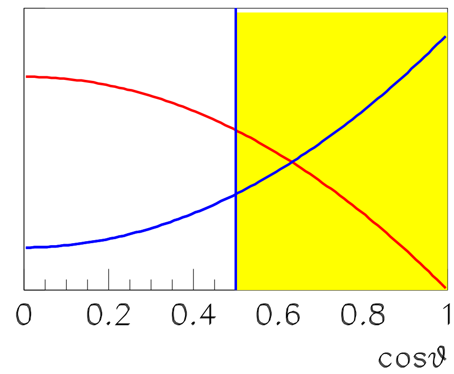

Fitting model.

☐ Background model:

$$B(m) = P(m)e^{a_1 m + a_2 m^2} \; for \; m < m_0$$

$$B(m) = P(m)e^{b_0 + b_1 m + b_2 m^2} \; for \; m > m_0$$

where $P(m)$ is the two-body phase space.

b_0 and b_1 are obtained by imposing continuity on the function and its first derivative.

☐ Use relativistic Breit-Wigner for $D_2^*(2460)$ and $D_0^*(2400)$ decaying to $D\pi$.

☐ Simple Breit-Wigner are used for the other structures.

☐ Each Breit-Wigner is multiplied by the phase-space factor.

☐ The cross-feed lineshapes from $D_1(2420)$ and $D_2^*(2460)$ appearing in the $D^+\pi^-$ and $D^0\pi^+$ mass spectra are described by a Breit-Wigner function fitted to the data.

Fit to the *Enhanced Unnatural Parity Sample*.

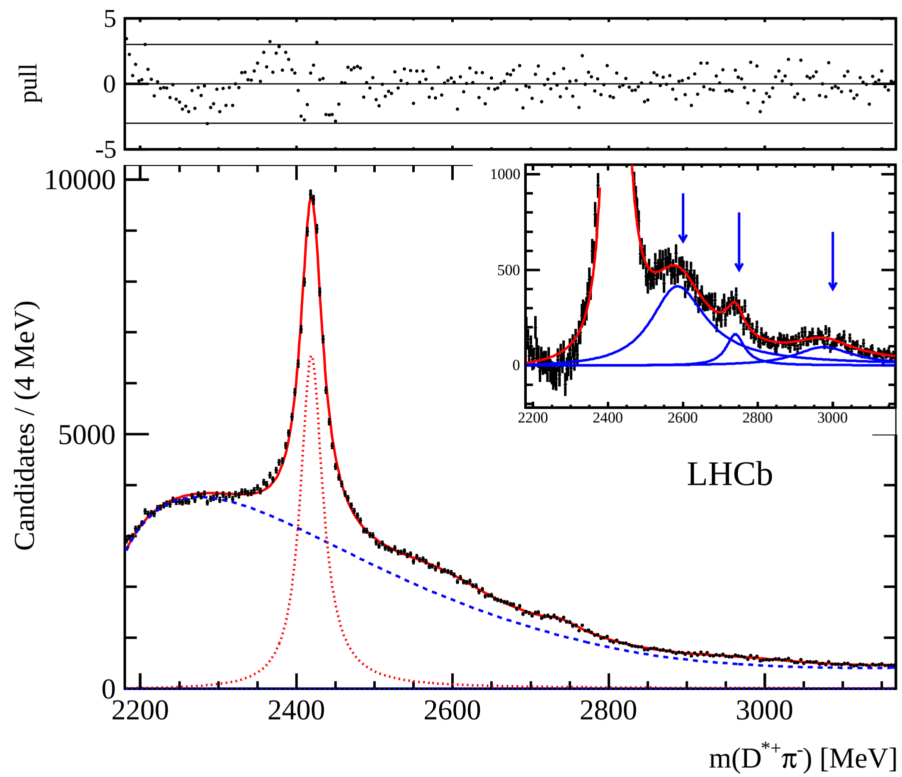

- We expect Natural Parity consistent with zero.
- $D_2^*(2460)^0$ yield consistent with zero.
- Observe $D_1(2420)^0$.
- **Observe three further structures:**

$$D_J(2580)^0, D_J(2740)^0, D_J(3000)^0$$

Fit to the ***Natural Parity Sample*.**

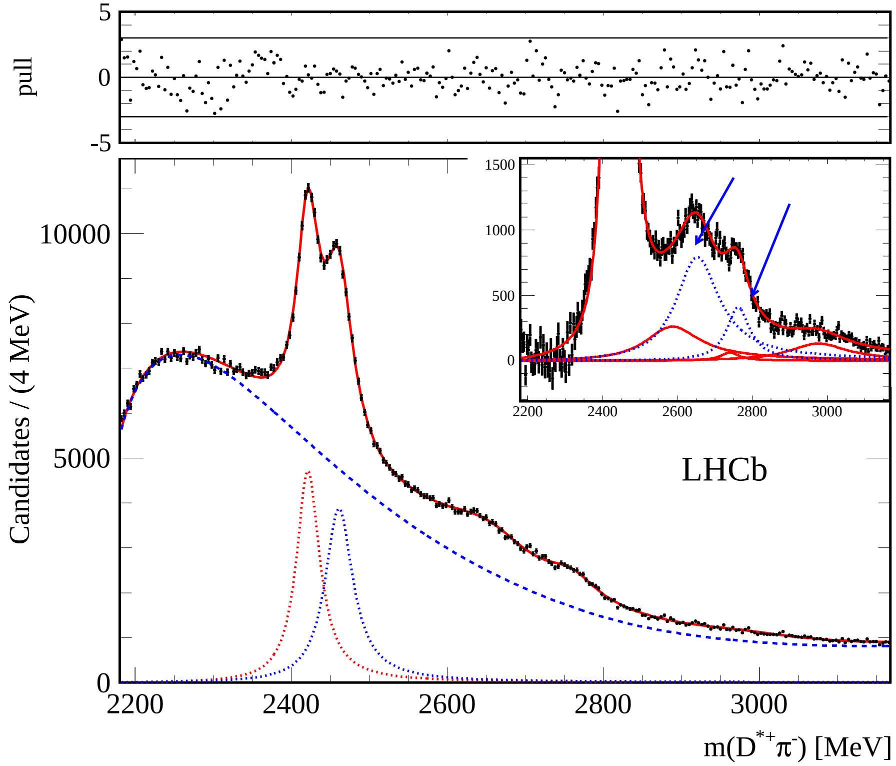

- We expect Enhanced Natural Parity contributions.
- Observe $D_1(2420)^0$ and $D_2^*(2460)^0$.
- Fix the $D_J(2580)^0$, $D_J(2740)^0$, and $D_J(3000)^0$ parameters.
- **Observe two further structures:**

$$D_J^*(2650)^0, D_J^*(2760)^0$$

Fit to the *Unnatural Parity Sample* and *Total Sample*.

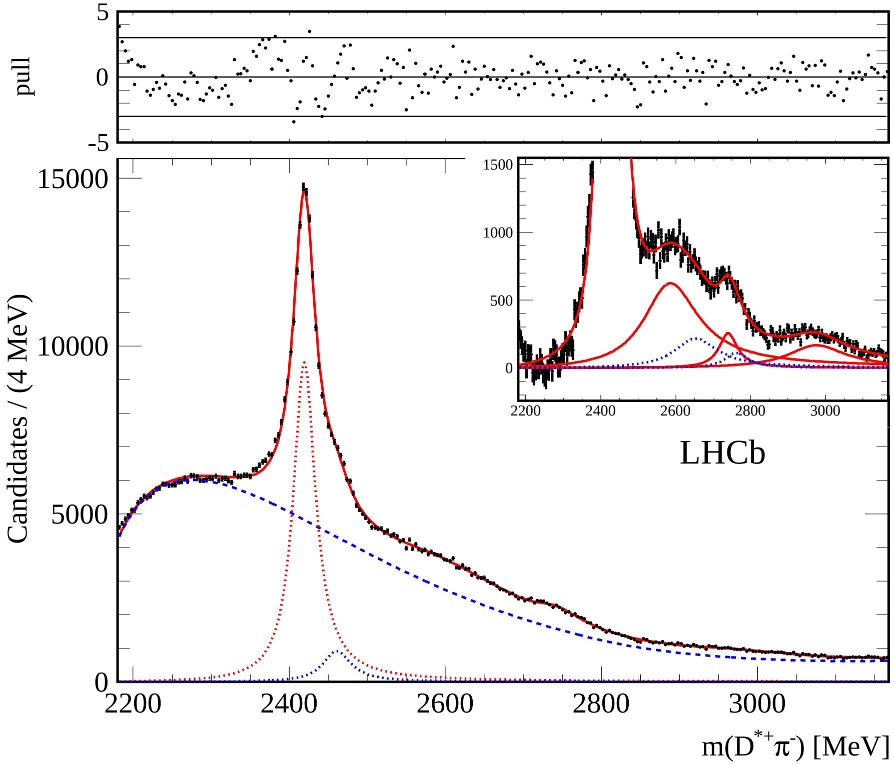

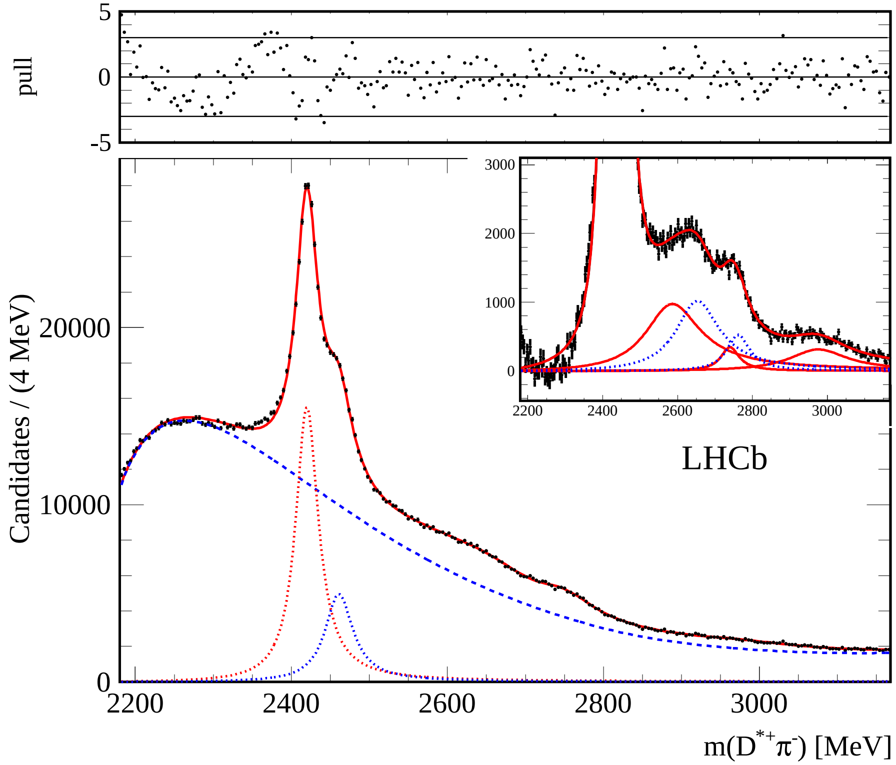

- Unnatural Parity Sample: fix all resonances parameters except for $D_1(2420)^0$.
- Total: all resonances parameters fixed.

Angular distributions (1).

- Divide the $D^{*+}\pi^-$ sample into 10 equally-spaced $cos\theta_H$ slices.
- Fit the mass spectra with fixed resonances parameters. Obtain yields.
- Plot yields as functions of $cos\theta_H$ for the different resonances.

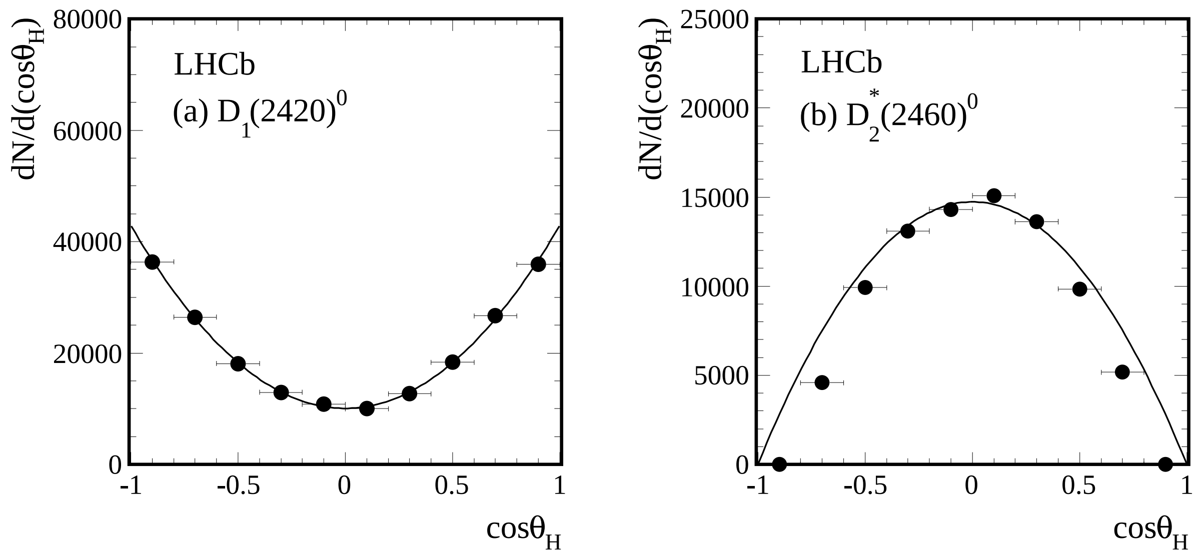

- $D_1(2420)^0$ has $J^P = 1^+$. Fitted with $1 + hcos^2\theta_H$, $h = 3.30 \pm 0.48$. $\chi^2/\text{ndf} = 0.67/8$
- $D_2^*(2460)^0$ has $J^P = 2^+$. Fitted with $sin^2\theta_H$. $\chi^2/\text{ndf} = 8.5/9$

Angular distributions (2).

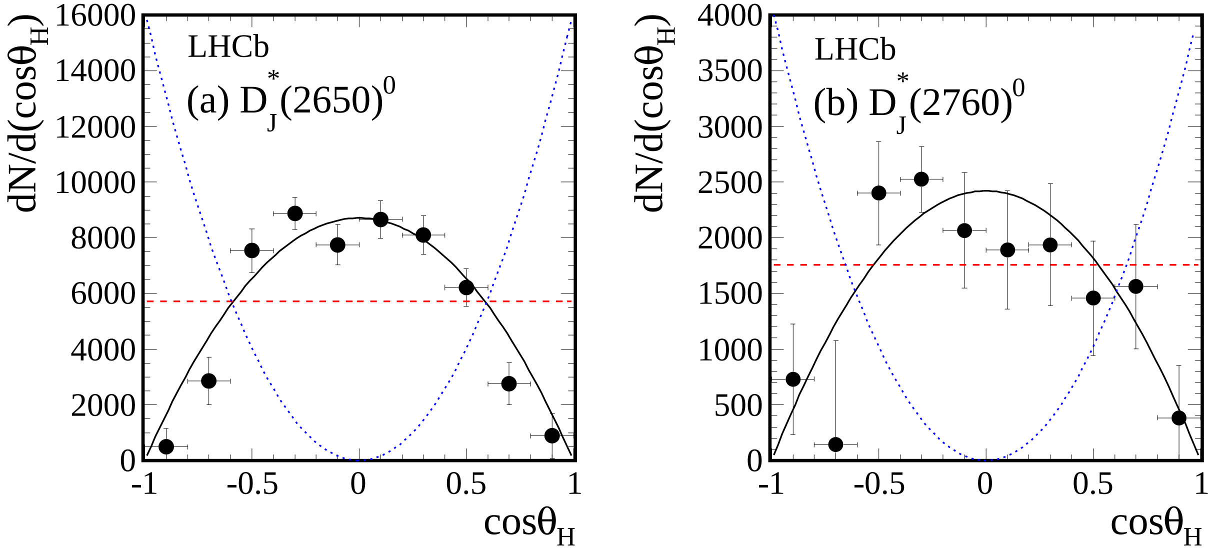

□ $D_J^*(2650)^0$ and $D_J^*(2760)^0$ are consistent with having Natural Parity.

□ Fitted with $sin^2\theta_H$. $\chi^2/\text{ndf} = 6.8/9$ and $\chi^2/\text{ndf} = 5.8/9$ respectively.

(black: natural parity), *(dashed red: unnatural parity)*, *(dotted blue: $J^P = 0^-$)*

Angular distributions (3).

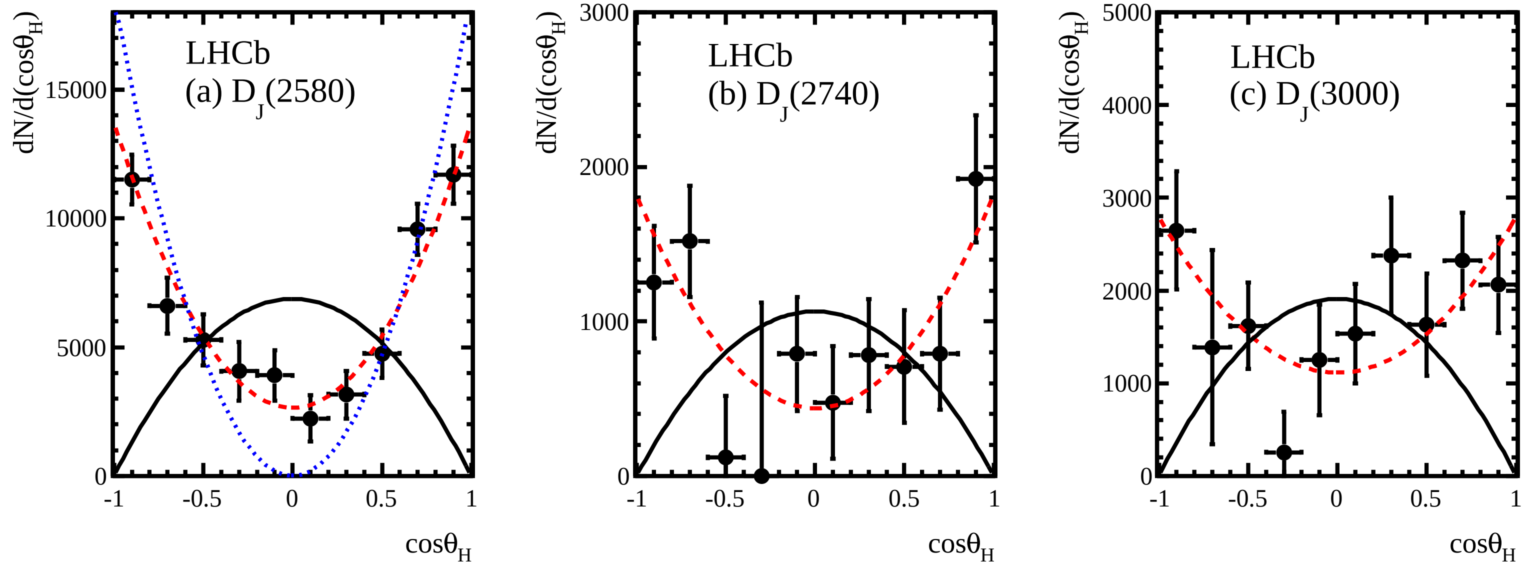

□ $D_J(2580)^0$, $D_J(2740)^0$, and $D_J(3000)^0$ are consistent with having Unnatural Parity. Fitted with $1 + hcos^2\theta_H$.

□ $\chi^2/\mathrm{ndf} = 3.4/8$, $\chi^2/\mathrm{ndf} = 6.6/8$ and $\chi^2/\mathrm{ndf} = 10/8$, respectively.

(black: natural parity), *(dashed red: unnatural parity)*,

(dotted blue: $J^P = 0^-$, $\chi^2/\mathrm{ndf} = 23/9$)

Cross-feeds into the $D\pi$ final states.

☐ We normalize the $D^{*+}\pi^-$ and $D^+\pi^-$ mass spectra using the sum of the $D_1(2420)^0$ and $D_2^*(2460)^0$ signals and obtain:

$$N(D^+\pi^-) = N(D^{*+}\pi^-) \cdot R_{D^+\pi^-}, \qquad R_{D^+\pi^-} = 1.41 \pm 0.02$$

☐ Similarly for the $D^0\pi^+$ final state.

$$N(D^0\pi^+) = N(D^{*+}\pi^-) \cdot R_{D^0\pi^+}, \qquad R_{D^0\pi^+} = 1.87 \pm 0.02$$

☐ We compute MC cross-feeds into the $D\pi$ from the new resonances observed in the $D^{*+}\pi^-$ mass spectrum using the above normalizations.

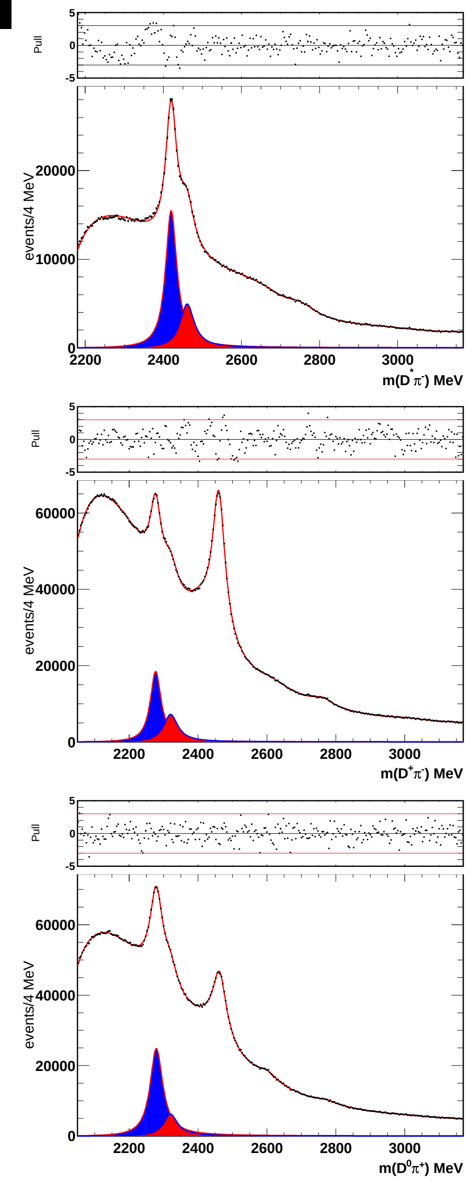

Fit to the $D^+\pi^-$ and $D^0\pi^+$ mass spectra.

□ Cross-feeds (in red) produce a distortion of the $D_2^*(2460)$ and $D_J^*(2650)$ lineshapes.

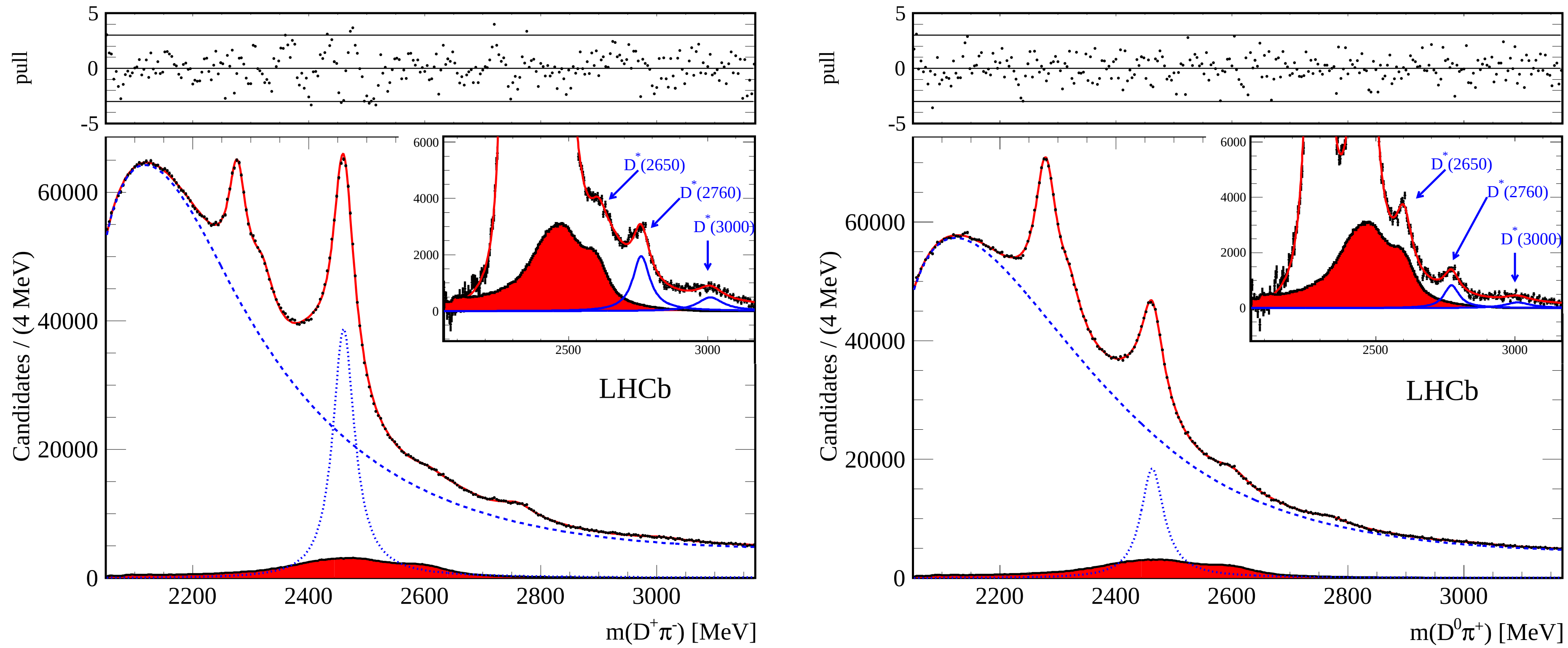

□ For $D_J^*(2650)$ we rely on the results obtained from the $D^{*+}\pi^-$ mass analysis.

□ We observe the $D_J^*(2760)$.

□ The fits requires the presence of a broad structure around 3.0 GeV which we label $D_J^*(3000)$.

Resulting resonances parameters, yields and significances.

Resonance	Final state	Mass (MeV)	Width (MeV)	Yields $\times 10^3$	Sign.
$D_1(2420)^0$	$D^{*+}\pi^-$	$2419.6 \pm 0.1 \pm 0.7$	$35.2 \pm 0.4 \pm 0.9$	$210.2 \pm 1.9 \pm 0.7$	
$D_2^*(2460)^0$	$D^{*+}\pi^-$	$2460.4 \pm 0.4 \pm 1.2$	$43.2 \pm 1.2 \pm 3.0$	$81.9 \pm 1.2 \pm 0.9$	
$D_J^*(2650)^0$	$D^{*+}\pi^-$	$2649.2 \pm 3.5 \pm 3.5$	$140.2 \pm 17.1 \pm 18.6$	$50.7 \pm 2.2 \pm 2.3$	24.5
$D_J^*(2760)^0$	$D^{*+}\pi^-$	$2761.1 \pm 5.1 \pm 6.5$	$74.4 \pm 3.4 \pm 37.0$	$14.4 \pm 1.7 \pm 1.7$	10.2
$D_J(2580)^0$	$D^{*+}\pi^-$	$2579.5 \pm 3.4 \pm 5.5$	$177.5 \pm 17.8 \pm 46.0$	$60.3 \pm 3.1 \pm 3.4$	18.8
$D_J(2740)^0$	$D^{*+}\pi^-$	$2737.0 \pm 3.5 \pm 11.2$	$73.2 \pm 13.4 \pm 25.0$	$7.7 \pm 1.1 \pm 1.2$	7.2
$D_J(3000)^0$	$D^{*+}\pi^-$	2971.8 ± 8.7	188.1 ± 44.8	9.5 ± 1.1	9.0
$D_2^*(2460)^0$	$D^+\pi^-$	$2460.4 \pm 0.1 \pm 0.1$	$45.6 \pm 0.4 \pm 1.1$	$675.0 \pm 9.0 \pm 1.3$	
$D_J^*(2760)^0$	$D^+\pi^-$	$2760.1 \pm 1.1 \pm 3.7$	$74.4 \pm 3.4 \pm 19.1$	$55.8 \pm 1.3 \pm 10.0$	17.3
$D_J^*(3000)^0$	$D^+\pi^-$	3008.1 ± 4.0	110.5 ± 11.5	17.6 ± 1.1	21.2
$D_2^*(2460)^+$	$D^0\pi^+$	$2463.1 \pm 0.2 \pm 0.6$	$48.6 \pm 1.3 \pm 1.9$	$341.6 \pm 22.0 \pm 2.0$	
$D_J^*(2760)^+$	$D^0\pi^+$	$2771.7 \pm 1.7 \pm 3.8$	$66.7 \pm 6.6 \pm 10.5$	$20.1 \pm 2.2 \pm 1.0$	18.8
$D_J^*(3000)^+$	$D^0\pi^+$	3008.1 (fixed)	110.5 (fixed)	7.6 ± 1.2	6.6

□ Significances are evaluated as $\sqrt{\Delta\chi^2}$ where $\Delta\chi^2$ is the difference between the χ^2 values when a resonance is included or excluded from the fit.

□ Significances are all above 5σ.

□ We do not evaluate systematic uncertainties on the parameters of the $D_J^*(3000)/D_J(3000)$ structures because at the edge of the mass spectra.

Discussion (1).

- We observe, in the $D^{*+}\pi^-$ mass spectrum, $D_1(2420)^0$ and measure its spin-parity consistent with $J^P = 1^+$.
- We observe, in the $D^{*+}\pi^-$ and $D^+\pi^-$ mass spectra, the $D_2^*(2460)^0$ resonance and find its spin-parity consistent with $J^P = 2^+$.
- We also observe the $D_2^*(2460)^+$ resonance in the $D^0\pi^+$ mass spectrum.

Discussion (2).

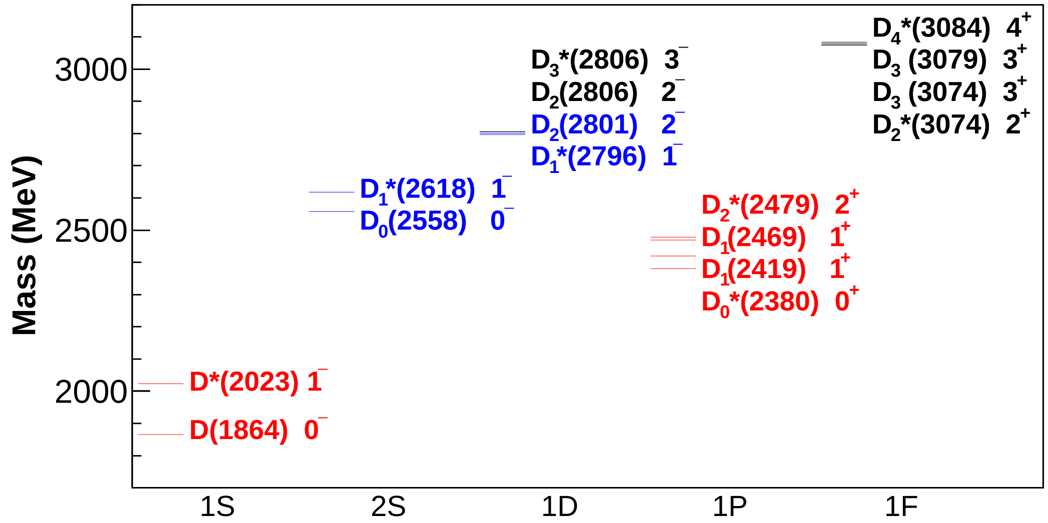

- The $D_J^*(2650)^0$ resonance could be identified as a $J^P = 1^-$ state (2S $D_1^*(2618)$).
- The $D_J^*(2760)^0$ could be identified as a $J^P = 1^-$ state (1D $D_1^*(2796)$).
- The $D_J(2580)^0$ could be identified with the (2S $D_0(2558)$) state, although $J^P = 0^-$ does not fit well the data.
- The $D_J(2740)^0$ could be identified as the $J^P = 2^-$ (1D $D_2(2801)$) resonance.
- Broad structures are observed around 3.0 GeV in the $D^{*+}\pi^-$ and $D\pi$ mass spectra. They could be superpositions of several states.

Excited D_s states.

- Experimental status of the D_s mesons.

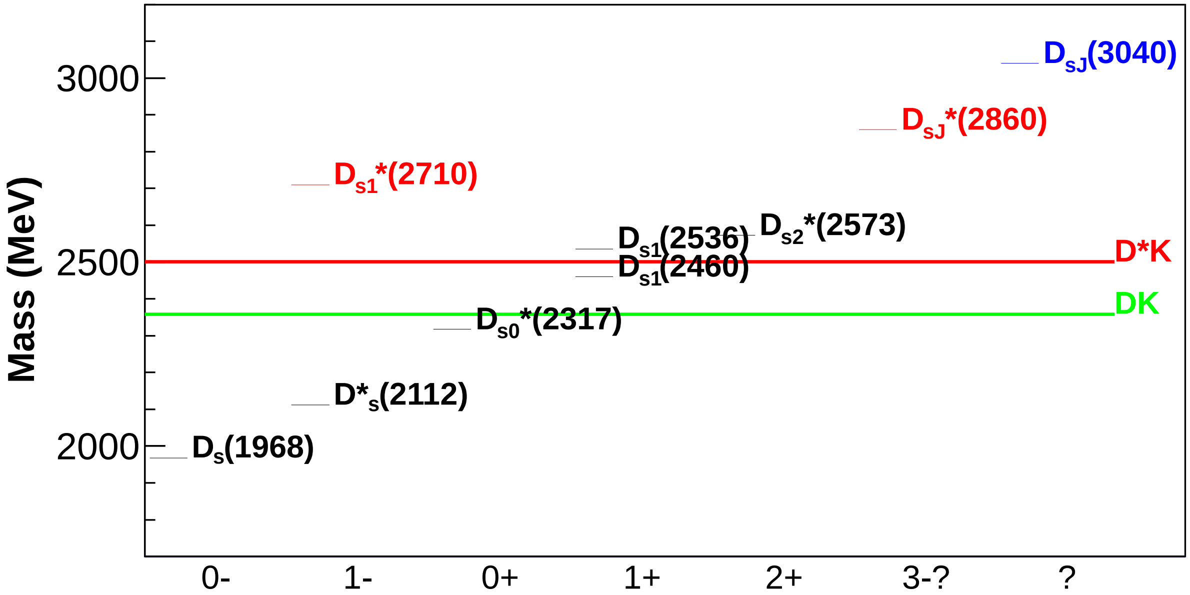

- Large discrepancy between predictions and experiment for $D^*_{s0}(2317)$ and $D_{s1}(2460)$.
- $D^*_{s1}(2710)$ observed by BaBar (inclusive) and Belle (B decays).
- $D^*_{sJ}(2860)$ and $D_{sJ}(3040)$ observed by BaBar.
- Controversial spin assignment for $D^*_{sJ}(2860)$. Overlap of two states?

Study of Excited D_s states in LHCb.

- We reconstruct the following final states ($1.0\,\text{fb}^{-1}$ of data)(JHEP1210(2012)151):

$$\mathbf{pp} \rightarrow \mathbf{X} \quad \mathbf{K^0_S D^+}_{\rightarrow K^-\pi^+\pi^+}, \quad \mathbf{pp} \rightarrow \mathbf{X} \quad \mathbf{K^+ D^0}_{\rightarrow K^-\pi^+}$$

- Similar strategy as in the $D^{(*)}\pi$ analysis.

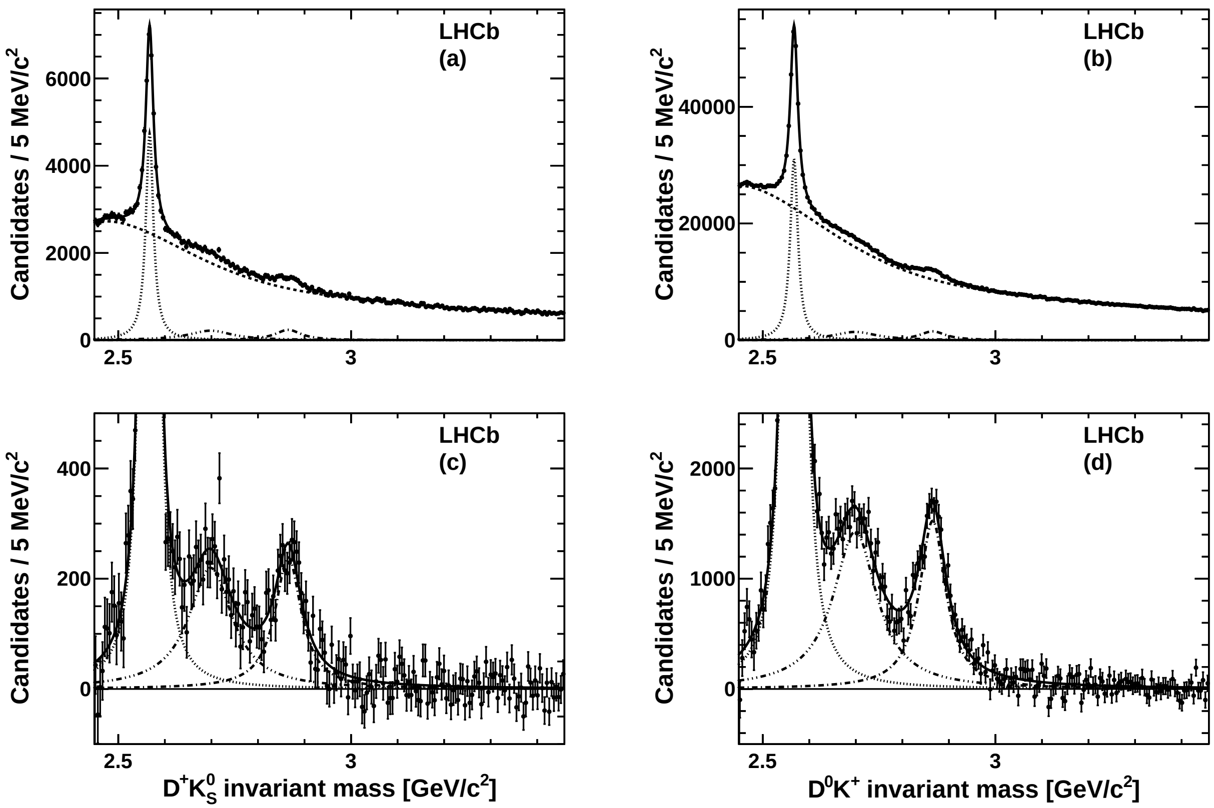

- First observation of $D^*_{s1}(2710)^+$ and $D^*_{sJ}(2860)^+$ in hadronic collisions.

$D^*_{s1}(2710)^+$ and $D^*_{sJ}(2860)^+$ parameters.

$$
\begin{aligned}
m(D^*_{s1}(2710)^+) &= 2709.2 \pm 1.9(\text{stat}) \pm 4.5(\text{syst})\ \text{MeV}/c^2, \\
\Gamma(D^*_{s1}(2710)^+) &= 115.8 \pm 7.3(\text{stat}) \pm 12.1(\text{syst})\ \text{MeV}/c^2, \\
m(D^*_{sJ}(2860)^+) &= 2866.1 \pm 1.0(\text{stat}) \pm 6.3(\text{syst})\ \text{MeV}/c^2, \\
\Gamma(D^*_{sJ}(2860)^+) &= 69.9 \pm 3.2(\text{stat}) \pm 6.6(\text{syst})\ \text{MeV}/c^2.
\end{aligned}
$$

□ Resonances observed in BaBar and Belle have been confirmed. All results are in agreement.

□ The statistical uncertainties for all parameters are improved by an overall factor of two with respect to the BaBar measurements in the same decay modes.

□ An angular analysis of D^*K samples is needed.

Measurement of the D masses.

- ☐ Use low Q-value modes: $D^0 \to K^- K^+ K^- \pi^+$, $D^0 \to K^- K^+ \pi^- \pi^+$ and $D_{(s)} \to K^+ K^- \pi^+$.
- ☐ Main systematics from momentum scale and energy loss correction.
- ☐ Calibrate momentum scale using $B^+ \to J/\psi K^+$ and $B^+ \to J/\psi K^+ \pi^+ \pi^-$.
- ☐ LHCb measurements using 1 fb^{-1} (JHEP 06 (2013), 065).

$$
\begin{aligned}
M(D^0) &= 1864.75 \pm 0.15\,(\text{stat}) \pm 0.11\,(\text{syst})\ \text{MeV}/c^2, \\
M(D^+) - M(D^0) &= 4.76 \pm 0.12\,(\text{stat}) \pm 0.07\,(\text{syst})\ \text{MeV}/c^2, \\
M(D_s^+) - M(D^+) &= 98.68 \pm 0.03\,(\text{stat}) \pm 0.04\,(\text{syst})\ \text{MeV}/c^2.
\end{aligned}
$$

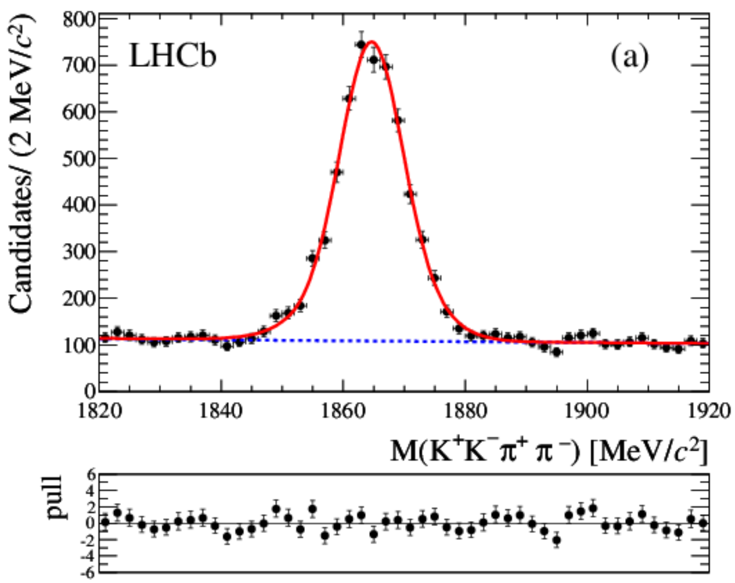

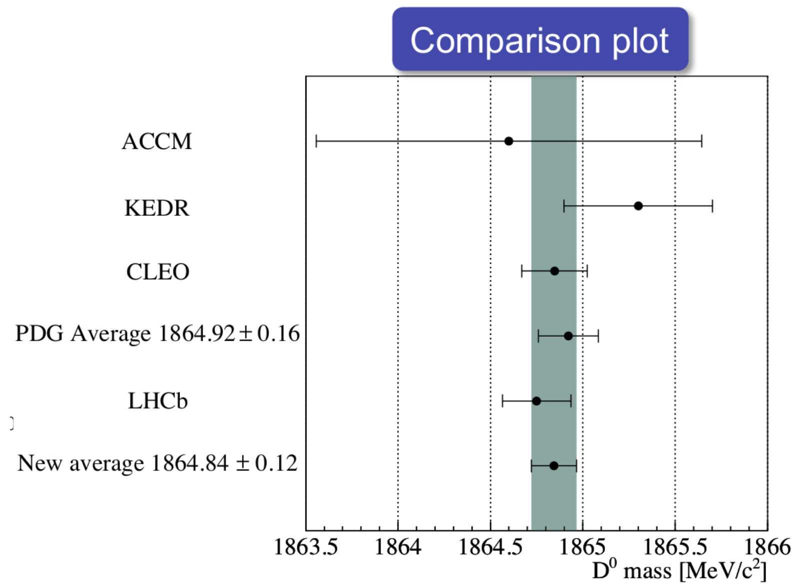

- ☐ Very recent BaBar measurement: $M(D^0) = 1864.841 \pm 0.048 \pm 0.063$ (arXiv:1308.1151).

Measurement of the D^+ and D_s^+ mass differences.

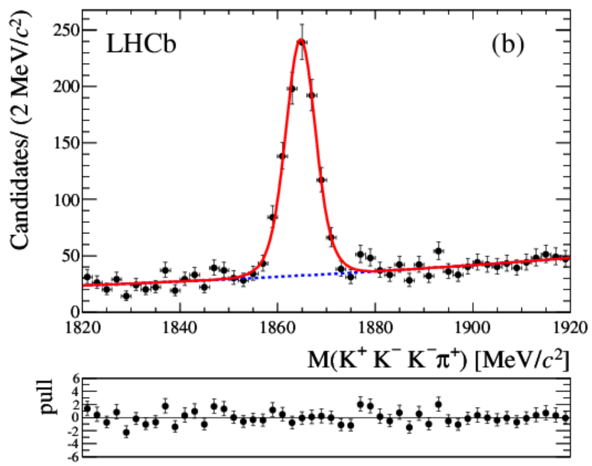

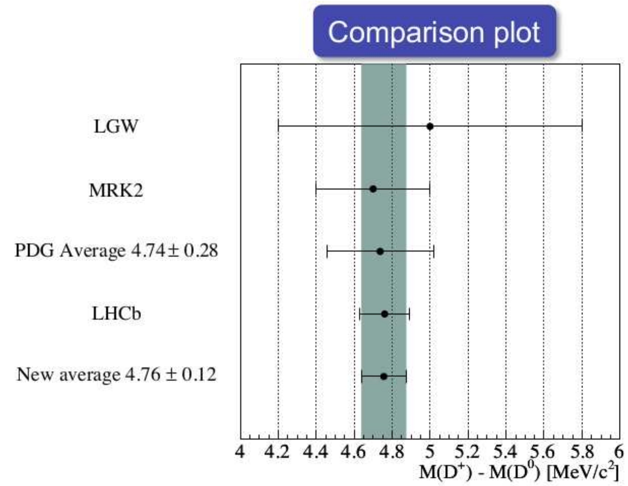

□ Factor 3 better than PDG measurements.

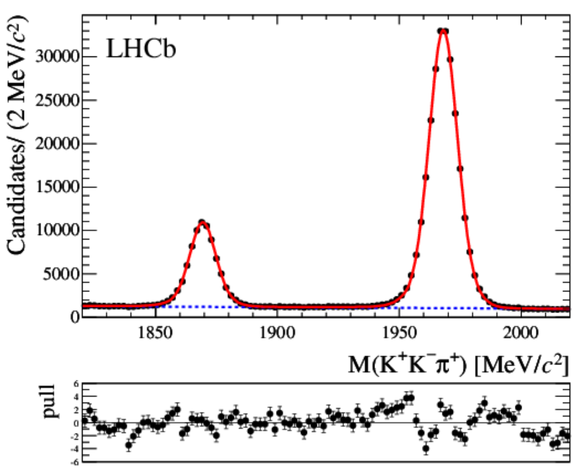

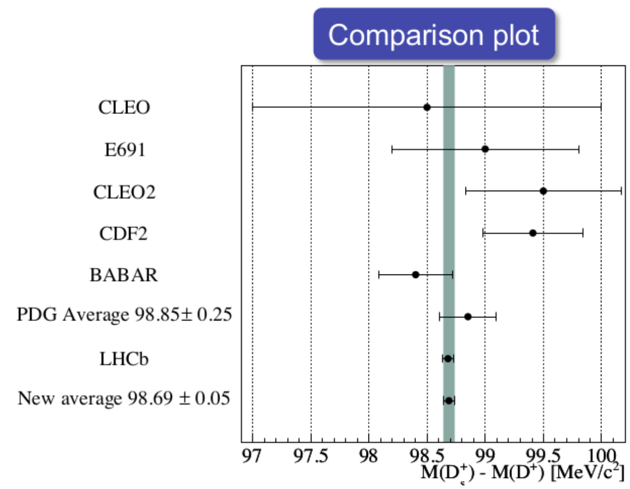

□ Factor 5 better than PDG average.

Conclusions.

□ Charm spectroscopy has made important progress at LHCb.

□ In the sector of the D_J spectroscopy we observe two new natural parity and two new unnatural parity resonances to be compared with previous measurements from BaBar.

□ We also observe further structures in the 3000 MeV mass region.

□ In the sector of the D_{sJ} spectroscopy we confirm, with higher statistics, results obtained at B factories and therefore $D^*_{s1}(2710)$ and $D^*_{sJ}(2860)$ are now "established".

□ Other analyses are in progress.

□ In the near future, we expect new results from the study of B and B_s decays.

□ In these exclusive decays will be possible to perform spin analysis and measurements of branching fractions.

Backup.

Optimization.

- □ Invariant massses computed as mass diferences. For example $m(D^+\pi^-)$ is defined as: $m(D^+\pi^-) = m(K^-\pi^+\pi^+\pi^-) - m(K^-\pi^+\pi^+) + m_{D^+}(PDG)$
- □ Signal/background ratio for the observed resonances improves with $p_T(D^{(*)}\pi)$.
- □ For the $D^+\pi^-$ mass spectrum we optimize on the strong $D_2^*(2460)^0$ signal.
- □ Fit the $D^+\pi^-$ mass spectrum with increasing p_T cut. Compute:

$Purity(P) = Signal/(Signal + Background),$

$Significance(S) = Signal/\sqrt{Signal + Background},$

$Product: \; S \cdot P$

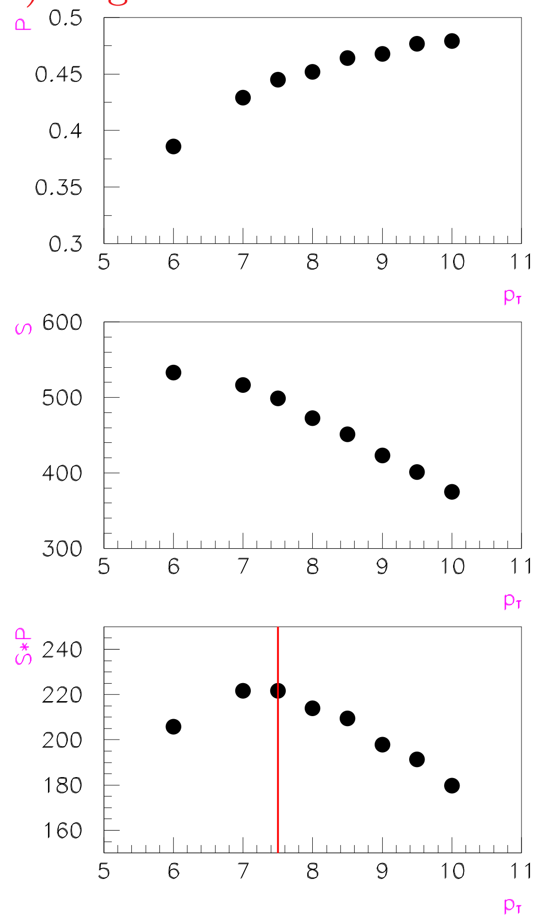

- □ **Choose a cut at $p_T > 7.5$ GeV/c for all final states.**
- □ No improvement is found as a function of the pseudorapidity.
- □ After the optimization 7.9×10^6, 7.5×10^6 and 2.1×10^6 $D^+\pi^-$, $D^0\pi^+$ and $D^{*+}\pi^-$ candidates are obtained.

Fits quality, cross checks and systematic uncertainties

- Summary of the fits to the different mass spectra.

Final state	Selection	Fit Range (MeV)	Number of bins	Candidates ($\times 10^6$)	χ^2/ndf
$D^+\pi^-$	Total	2050-3170	280	7.90	551/261
$D^0\pi^+$	Total	2050-3170	280	7.50	351/262
$D^{*+}\pi^-$	Total	2180-3170	247	2.04	438/234
$D^{*+}\pi^-$	*Natural parity sample*			0.98	263/229
$D^{*+}\pi^-$	*Unnatural parity sample*			1.06	364/234
$D^{*+}\pi^-$	*Enhanced unnatural parity sample*			0.55	317/230

- Cross checks on the fits results and stability have been performed.
  - The p_T cut has been lowered to 7.0 GeV/c: results are in agreement within the statistical errors.
  - For each mass spectrum we generate and fit 500 new mass spectra obtained by Poisson fluctuations of each bin content.
- The following systematic uncertainties have been evaluated on the resonances masses and yields.
  - We make use of different background models.
  - For each mass spectrum we generate and fit 500 new mass spectra with resonances and background yields fixed to the fit results. The background parameters are allowed to vary within $\pm 3\sigma$ from the fitted values.
  - In the $D\pi$ mass spectra the simple Breit-Wigner are replaced by relativistic BW.
  - Fixed parameters resonances have been relaxed one by one.